Soft Computing (2021) 25:10953–10968
https://doi.org/10.1007/s00500-021-05811-4

APPLICATION OF SOFT COMPUTING

Design and development of an adaptive-torque-based proportional-integral-derivative controller for a two-legged robot

Ravi Kumar Mandava[1] · Pandu R. Vundavilli[2]

Accepted: 8 April 2021 / Published online: 20 April 2021

Abstract

The torque-based proportional-integral-derivative (PID) controller proposed in this paper is operated on joint motors by minimizing the error between the target and actual angular displacements of that joint to achieve a superior control. On the basis of the aforementioned phenomenon, the execution effectiveness of the two-legged robot's gait can be controlled. The PID controller parameter tuning is a laborious and time-consuming process, and the controllers' performance depends on the gain values set for the controller. To overcome the said drawbacks, this study develops an adaptive-torque-based PID controller for a two-legged robot that can provide adaptive gains on the basis of the magnitude of input signal received at the input nodes of the neural network (NN). Furthermore, the structure of the feedforward NN has been optimized with the help of the modified chaotic invasive weed optimization (MCIWO) algorithm. Moreover, the concept of zero moment point has been employed to check the balance of the two-legged robot while walking on various terrains (that is, flat, stair, and sloped surfaces). The effectiveness of the developed controller has been verified in both simulations and practical.

Keywords Two-legged robot · Adaptive · PID controller · MCIWO-NN · Zero moment point

Nomenclature

b	Number of intervals considered in one step
d	Number of training scenarios
e	Error at two consequent joints
f	Fitness of the current colony
f_{max} and f_{min}	Maximum and minimum fitness
f_s	Foot length of the two-legged robot (m)
f_w	Foot width of the two-legged robot (m)
g	Acceleration due to gravity (m/sec^2)
G	Gravity terms in torque equation
Gen_{max}	Maximum no. of generations
h	Centrifugal/Coriolis terms in torque equation
H_1	Swing leg hip height (m)
K_p	Proportional gain
K_d	Derivative gain
K_i	Integral gain
$l_1, l_2 \ldots l_{18}$	Length of the limbs (m)
L_1	Distance between the swing leg ankle joint and hip joint (m)
$m_1, \ldots m_{18}$	Mass of the links (kg)
M	Inertia terms in torque equation
p	Number of joints for which the controllers are designed
$I_1 \ldots I_{18}$	Moment of Inertia of the links (kg-m^2)
$r_1, \ldots r_{18}$	Distance between the mass center and one edge of the link (m)
S	Number of seeds
S_{max} and S_{max}	Maximum and minimum no. of seeds

Greek Symbols

$\theta_1 \ldots \theta_{18}$	Joint angles between different links (m)
τ_{the}	Theoretical torque (N-m)
τ_{act}	Actual torque (N-m)
$\sigma_{initial}$	Standard deviation at initial position
σ_{final}	Standard deviation at final position
σ	Standard deviation

Abbreviation

DBM	Dynamic balance margin

✉ Ravi Kumar Mandava
rm19@iitbbs.ac.in

Pandu R. Vundavilli
pandu@iitbbs.ac.in

[1] Department of Mechanical Engineering, MANIT Bhopal, Bhopal 462003, India

[2] School of Mechanical Sciences, IIT Bhubaneswar, Bhubaneswar 752050, India

MCIWO	Modified chaotic invasive weed optimization
PSO	Particle swarm optimization
DE	Differential Evaluation
NN	Neural network
PID	Proportional integral and derivative
ZMP	Zero moment point

1 Introduction

Robotic systems are extensively used in various complex engineering applications, where the demand for productivity, performance and safety during the operation is very high. Therefore, two-legged robots are used in non-industrial environments such as assisting doctors in hospitals and performing various tasks in hotels and industrial environments such as nuclear reactors, boilers clean-up, and space applications. A two-legged robot can walk on numerous surfaces such as flat, staircases, sloped surfaces, surfaces with ditches and roads made of sand and small stones in a real environment. However, it is challenging to make the two-legged robot accomplish the aforementioned tasks in a systematic manner on various terrains. In such situations, the controller plays a key role in enhancing the balance of the two-legged robot. On the other hand, tuning the gains of the proportional-integral-derivative (PID) controller in the field of control systems poses many problems, because the process is laborious and time consuming. In general, control system must be studied theoretically in the virtual domain by utilizing fewer assumptions and simplistic process. It is significant to note that the control problem related to the dynamic walking of the biped robot is more complicated than the static walking problem (Cheng and Lin 2000). In dynamic walking, the walking patterns are followed with a higher walking speed. Among all the above categories of walking patterns, the problem related to dynamically balanced walking is the most crucial and should be solved with a high degree of reliability. Finally, this question has motivated the formulation of several dynamically balanced criteria for obtaining balanced biped walk. The concept of zero moment point (ZMP) (Vukobratovic and Borovac 2004) was used by many researchers to obtain a dynamically balanced gait for a two-legged robot. To introduce more natural and stable walking pattern for a two-legged robot, Nguyen et al. (2016) proposed a novel gait generation method by using differential evaluation and artificial neural network algorithms. The authors had concluded that the developed method was easy and did not require much mathematical computations when compared with the conventional methods that used the concept of zero moment point. In Zang et al. (2016), the authors had developed a novel pneumatic musculoskeletal two-legged robot and proposed a suitable PID controller. There, the joints of lower limbs of the two-legged robot were driven by the muscles. This helped them to achieve the desired position for all joints. Further, to achieve the real-time stable walk for the two-legged robot, Kajita (2017) had proposed concept of inverted pendulum and its control by using a suitable feedback system.

PID controller tuning is an important process for autonomous robotic systems to complete the task assigned to them. Previously, many researchers focused on controlling robots by using a proportional and derivative controller (Slotine and Li 1991; Chu et al. 2008), PID controller (Shamna et al. 2017), computed torque controller (Kelly et al. 2005), energy efficient support vector machine learning controller (Wang 2013), adaptive controller (Yoo et al. 2007), fuzzy network (Hojati and Gazor 2002), neural network (NN) (Juang 2001), and fuzzy NN controller (Wai and Muthusamy 2013). Subsequently, a recurrent NN was used to compensate for the control signal of a seven-link two-legged robot (Wu et al. 2007). Furthermore, a novel foot force and body posture controllers were developed for a 42-DOF biped robot (Kajita 2010). The legged robotic system was considered as a humble linear inverted pendulum to solve the control problem. Moreover, a predictive-based PID controller that imitated the calculated time with reduced complexity to generate smooth and efficient walking was developed (Bouhajar et al. 2015). Note that some research was conducted on the dynamic balance of a two-legged robot by utilizing a ZMP-based regulator. Jimenez et al. (2013) developed an angular-momentum-based controller that increased the walking stability of the robot by using the preview control method for the ZMP. Moreover, a fuzzy control policy (Wu and Hwang 2011) was developed for a two-legged robot to generate dynamically balanced gaits while walking. To maintain ground contact, the authors used a simplified inverted pendulum model instead of the spring or damper ground model. Finally, the proposed controller was compared with the PID controller by conducting simulations and in practical. Furthermore, in a study, the stability of a two-legged robot was controlled using the ZMP-based trajectory controller (Aghbali and Koma 2013a), that is, PID and fuzzy controller with and without external disturbances. Here, the included angle made by the joints was set by an offline method. Moreover, an adaptive neuro PID controller was implemented by Anh et al. (2014) to optimize the gain scheduling and PID parameters of the multilayer feed forward NN. The algorithm was tested on a full size humanoid robot, and the algorithm's performance was observed to be better than that of the conventional PID controller. Koker et al. (2014) designed a neural network committee machine (NNCM) for solving the inverse

kinematics of a robotic manipulator. The developed method had shown better performance when compared with the results obtained from the algebraic, iterative and geometric approaches. Furthermore, Londhe and Patre (2018) developed an adaptive fuzzy sliding mode control for an autonomous underwater vehicle to achieve the robust trajectory tracking. Initially, the rules of the fuzzy controller were derived by using the Lyapunov energy function, which was used to minimize the chattering of the control signal. Finally, to enhance the stability of the system, an adaptive control law was established to adapt the fuzzy consequent parameter of a fuzzy logic controller. Alongside, for fine-tuning of the PID controller still researchers are using artificial neural network (Malekabadi et al. 2018) whose weights are tuned with the help of genetic algorithms. Moreover, Satoh and Fujimoto (2018) proposed a torso and knee trajectory learning and state-transition estimation method for generating the gait for the robot. They used a novel technique to generate the optimal gaits and to avoid the foot-scuffing problem. Clever et al. (2018) discussed the gait generation method used for the humanoid robot to move in complex environments. This method was based on the concept of template models and the optimality principles learned from the human beings.

After a through literature review, the contributions made in this research work are listed as follows:

- The ZMP-based PID controller used in most of the studies was replaced by a torque-based PID controller that helps in straight away reducing the error between the target and actual angular positions of various joints. However, the ZMP-based controller is not a direct method of regulating the motors. Moreover, there is no guarantee that the gaits produced by the ZMP-based PID controller are not going to exhibit the sequence-oriented gaits that fulfill the repeatability conditions.
- Most of the research work on the design of controller for a two-legged robot is pertained to decide the optimal values of the gains that are accountable for a smooth execution of the gaits designed by a gait planner. Note that the magnitude of error between the target and actual angular displacement is not the same during the control. These demands variation in the gain values to quickly minimize the error. However, this minimization cannot be obtained by using the optimal controller, because the obtained gain values are fixed during the process. This problem is eliminated using the proposed adaptive controller, because the NN performs the task of providing adaptive gains that correspond to the change in the magnitude of the error signal received at its input node.
- In the present study, a revised form of the invasive weed optimization procedure is proposed to train the NN's architecture that predicts the gains of the controller in an adaptive manner. The modification is performed by introducing the cosine and chaotic variables in the spatial dispersal phase. These variables enable the algorithm to enhance the search space and diminish the likelihood of trapping their solutions in the local optimum. To avoid computational complexity, the adaptive controller design for the lower limbs of the biped robot, which plays a major role while moving on various terrains, is only considered.

The present paper is structured as follows: The introduction related to the dynamics of the two-legged robot is presented in Sect. 2. Section 3 describes the adaptive controller, that is, the MCIWO-NN algorithm. The results related to the simulations and experiments are presents in Sect. 4. Finally, the conclusions are specified in Sect. 5.

2 Two-legged robot dynamics

The physical structure of the real two-legged robot used in this research is shown in Fig. 1. The dynamics associated with the two-legged robot have been determined by utilizing Lagrange–Euler (L–E) formulation. These L–E formulation is used to decide the required torques at numerous joints of the two-legged robot as mentioned below.

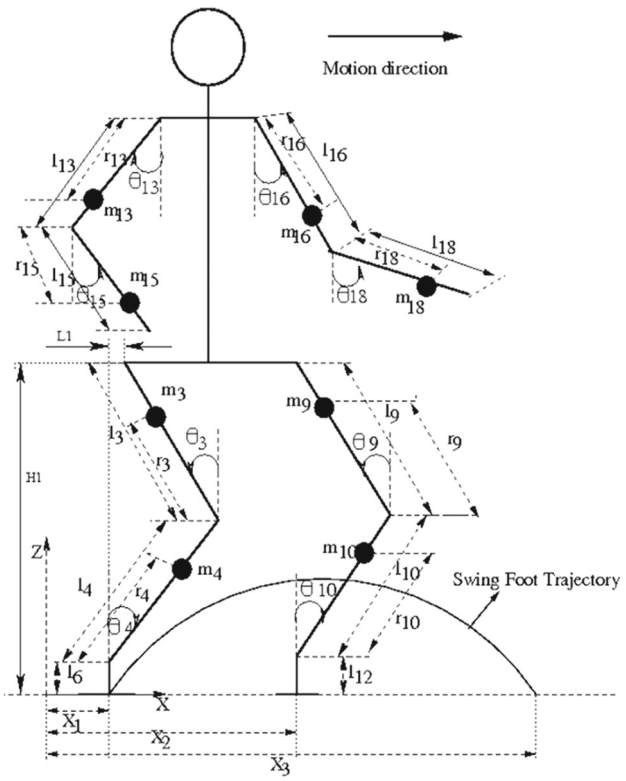

Fig. 1 Motion of the two-legged robot on flat surface

$$\tau_i = \sum_{j=1}^{n} M_{ij}(q)\dot{q} + \sum_{j=1}^{n}\sum_{k=1}^{n} h_{ijk}\dot{q}_j\dot{q}_k + G_i \quad i,j,k = 1\ldots n \tag{1}$$

where τ_i represents the torque required at joint i due to the motion of links, q denotes the movement (m) of the joint, $\dot{q}_j$ indicates the velocity (m/sec) of the joint, and $\dot{q}_j$ represents the acceleration (m/sec^2) of the joint. Furthermore, the enlarged form of inertia term, Coriolis/centrifugal term and gravity term are discussed below.

$$M_{ij} = \sum_{p=\max(i,j)}^{n} Tr\left[d_{pj} I_p d_{pi}^T\right] \quad i,j,k = 1\ldots n \tag{2}$$

$$h_{ijk} = \sum_{p=\max(i,j,k)}^{n} Tr\left[\frac{\partial\left(d_{pk}\right)}{\partial q_p} I_p d_{pi}^T\right] \quad i,j,k = 1\ldots n \tag{3}$$

$$G_i = -\sum_{p=i}^{n} m_p g d_{pi}\,{}^{p}\bar{r}_p \quad i,j,k = 1\ldots n \tag{4}$$

where I_p and ${}^{p}_{e}\bar{r}_p$ denote the moment of inertia tensor (Kg·m/sec^2) and mass center of the pth link (m), respectively, and 'g' indicates the acceleration due to gravity (m/sec^2).

3 Design of the PID controller

The controller has to play a main role on biped robots to maintain the dynamic balance. Moreover, the controller will supply the torque that is required by the individual joint to move from an initial position to final position. The main aim of the PID controller is to diminish the error between the actual process variable to the reference of the system. In the present research work, the authors developed a torque-based PID controller which will control all the joint motors individually. The required PID controller equation, which is helpful to control the joint motors individually, has been formulated after solving the dynamics of the two-legged robot and is given in Eq. 5.

$$\tau_{\text{act}} = K_p e(t) + K_p \frac{\mathrm{d}e(t)}{\mathrm{d}t} + K_i \int e(t)\mathrm{d}t \tag{5}$$

where $e(t)$ represents the error in the joint displacement and K_p, K_d, and K_i indicate the proportional, derivative, and integral gains of the controller. Further, the expanded form of Eq. (5) after inserting the meaning of $e(t)$ is given in Eq. (6) and (7).

$$e(\theta_i) = \theta_{if} - \theta_{is} \tag{6}$$

$$\tau_{i,\text{act}} = K_{pi}\left(\theta_{if} - \theta_{is}\right) - K_{di}\dot{\theta}_{is} + K_{ii}\int e(\theta_{is})\mathrm{d}t \quad i = 1\ldots n \tag{7}$$

where $\tau_{i,\text{act}}$ denotes the actual torque supplied by the individual motor to the joints for moving from an initial angular position (θ_{is}) to the final angular position (θ_{if}). The final control equation (ref. Equation 8) which is used to perform the control action for all joints.

$$\ddot{q}_j = \sum_{j=1}^{n} M_{ij}(q)^{-1}\left[-\sum_{j=1}^{n}\sum_{k=1}^{n} h_{ijk}\dot{q}_j\dot{q}_k - G_i\right] + K_{pi}\left(\theta_{if} - \theta_{is}\right) - K_{di}\dot{\theta}_{is} + K_{ii}\int e(\theta_{is})\mathrm{d}t \tag{8}$$

Moreover, the integral term in Eq. (8) should be replaced by its state variables and it is given in Eq. 9.

$$x_i = \int e(\theta_{is})\mathrm{d}t \cong \dot{x}_i = \theta_{if} - \theta_{is} \quad i = 1\ldots n \tag{9}$$

3.1 MCIWO-NN PID controller

The developed torque-based PID controller has been designed to achieve the stable walking of the biped robot on various terrains such as flat surface, ascending and descending the stair and sloping surfaces. Tuning of the PID controller using the manual process is a trial and error method, and it consumes more time. Further, the optimal PID controller provides only one set of optimal values for the proportional, integral, and derivative gains that are used by the controller to execute the gaits. To overcome these drawbacks, many researchers around the world are working on this problem. However, in the present research work, the authors present an adaptive controller (i.e. NN-based PID controller) that generates variable gains on the basis of the magnitude of the error signal. Moreover, to optimize the weights of the neural network structure, the authors used a novel optimization algorithm (i.e. MCIWO). The fitness of the NN can be enhanced by improving its structure by using MCIWO algorithm. Figure 2 displays the flowchart of operation of MCIWO-NN algorithm. The detailed description of the NN algorithm and MCIWO algorithm is discussed in the following subsections.

3.2 Neural network

The neural network consists of junctions which are connected with the help of simple processing units to process the data. The structure of the network (that is, shown in Fig. 3) consists of three layers, that is, input, hidden and output layers, and each layer consists of number of neurons. The weighted sum of the inputs and the bias values are added to each neuron, and the values are passed through transfer functions. The transfer functions, namely

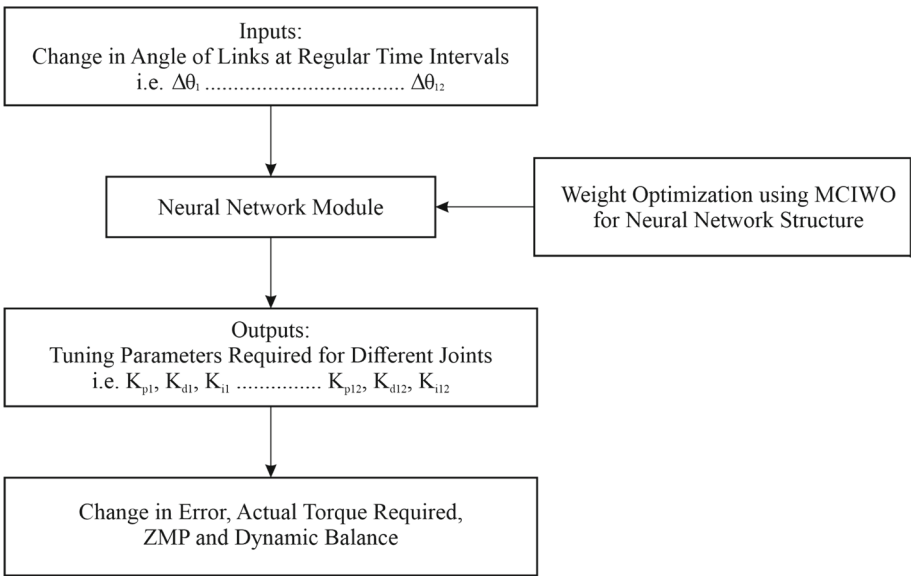

Fig. 2 Flowchart of the developed MCIWO-NN approach

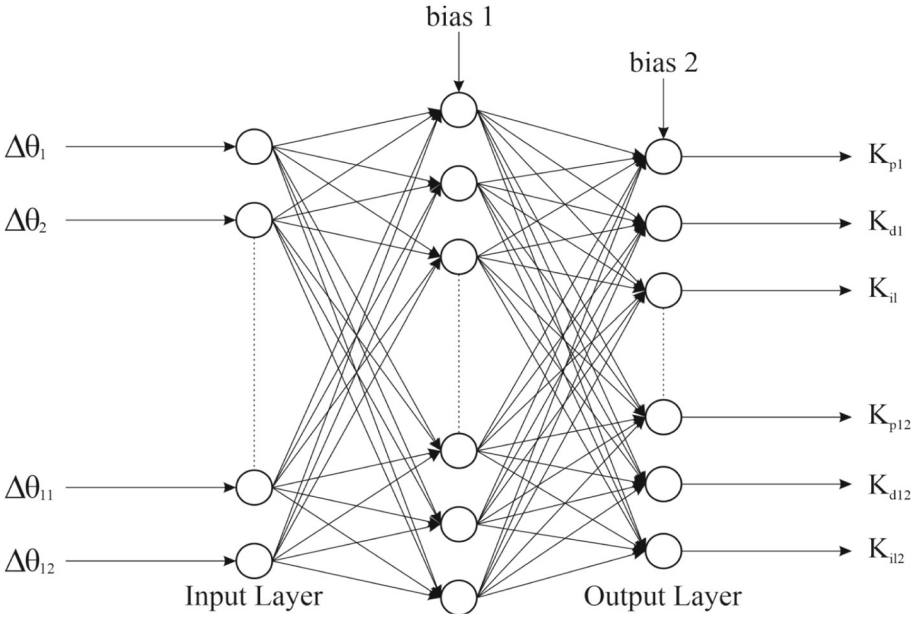

Fig. 3 Working structure of the NN

linear, log-sigmoid and tan-sigmoid functions, are assigned to the input, hidden and output layers, respectively. The error between the target and the actual angular displacement of various joints at different intervals is fed as inputs to the network (that is, $\Delta\theta_1$, $\Delta\theta_2$, $\Delta\theta_3$, $\Delta\theta_4$, $\Delta\theta_5$, $\Delta\theta_6$, $\Delta\theta_7$, $\Delta\theta_8$, $\Delta\theta_9$, $\Delta\theta_{10}$, $\Delta\theta_{11}$, and $\Delta\theta_{12}$). The gains of the PID controller, such as *Kp*, *Kd*, and *Ki*, for all the twelve controllers are considered as outputs of the network. The RMS deviation of the angular displacement between the end of each interval ($\propto_{ijkf}$) and the beginning of each interval ($\propto_{ijks}$) is considered as the fitness (f) of each population and is given below.

$$f = \frac{1}{d}\sum_{i=1}^{d}\left[\frac{1}{b}\sum_{j=1}^{b}\sqrt{\frac{1}{2}\sum_{k=1}^{p}\left(\alpha_{ijkf}-\alpha_{ijks}\right)^2}\right] \tag{10}$$

where '*d*' is the number of training scenarios, '*b*' is the number of intervals considered in one step, and '*p*' is the number of joints for which the controllers are designed.

3.3 Modified chaotic invasive weed optimization algorithm

The IWO is a nature inspired optimization algorithm introduced by Mehrabian and Lucas (2006), and it was motivated from the colonization phenomenon of invasive

weeds in nature. Moreover, it is a powerful optimization algorithm which can be formed by mimicking the properties of invasive weeds. The weed colonization behavior in a cropping field is explained in Fig. 4.

3.3.1 Initialization

Initially, a finite number of weeds are dispersed randomly in a D-dimensional space. In the present problem, the gains, i.e., K_p, K_d and K_i, are considered as weeds of the problem.

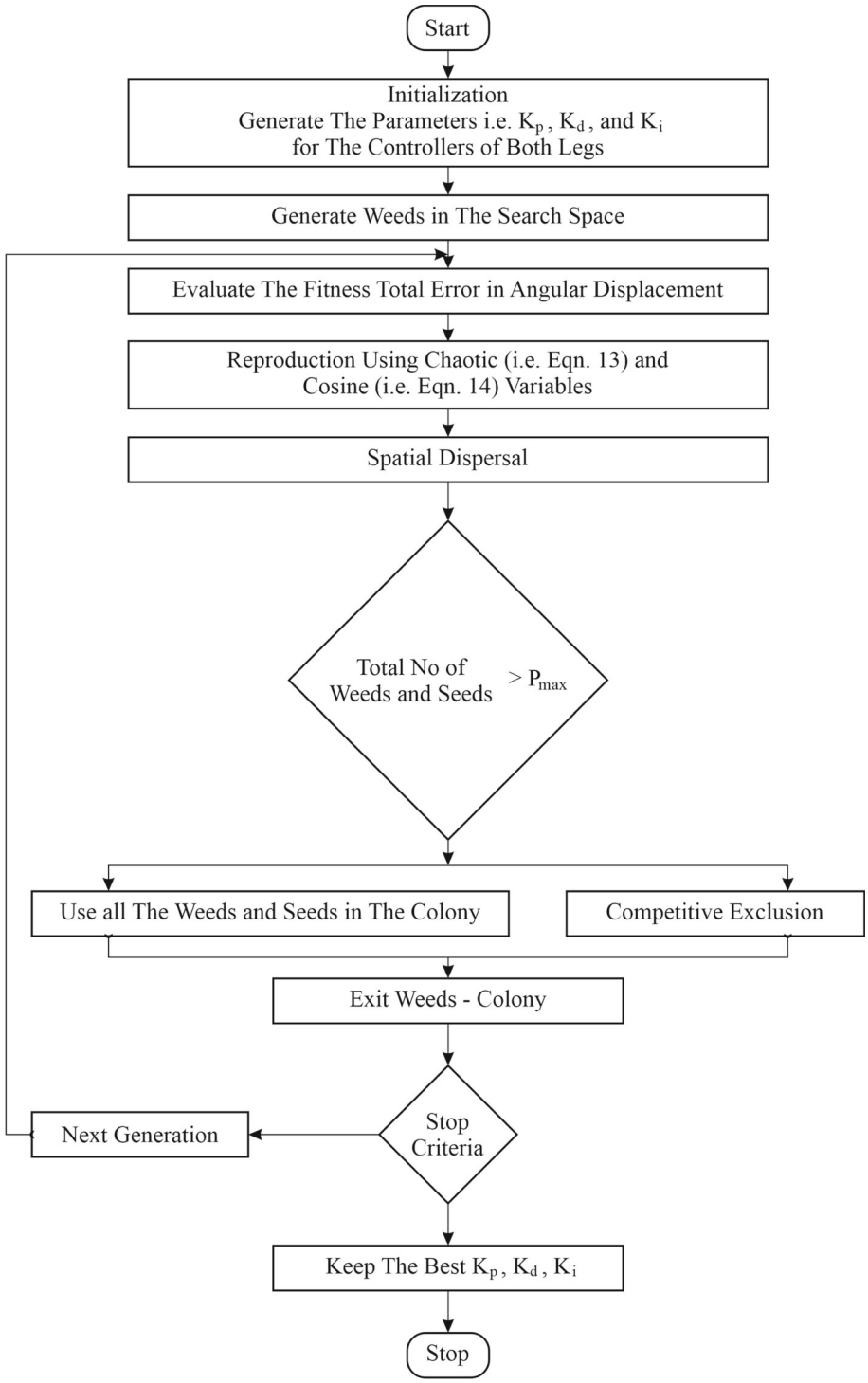

Fig. 4 Flowchart of the MCIWO algorithm operation

3.3.2 Reproduction

The dispersed weeds grow into flowering plants after using the unused resources and produce the new seeds. Further, the fitness of each plant will be evaluated based on the no. of seeds produced. In the present problem, the average angular positional error of the PID controllers is considered as the fitness. Once the fitness is evaluated, the process of reproduction starts to determine the number of seeds produced by the plant. The fitness of the weed is increased from the lower to higher in a linear manner on the basis of the number of seeds present in a weed (ref. Figure 5) (Naidu and Ojha 2015). A better fitness weed produces a high number of seeds, and the worst fitness weed produces the least number of seeds. The advantage of this algorithm is that all the weeds are participated in the solution space and to identify the weed with the less fitness value also it gives some useful information while in the evolution process (Affolter et al. 2016). Moreover, the number of produced seeds (S) which are generated by each weed is calculated using Eq. 11.

$$S = \text{Floor}\left[S_{\min} + \frac{f - f_{\min}}{f_{\max} - f_{\min}} \times S_{\max}\right] \tag{11}$$

where $f_{\min}$ and $f_{\max}$ represent the minimum and maximum fitness value in the colony, and $S_{\min}$ and $S_{\max}$ indicate the minimum and maximum production of each plant, respectively.

3.3.3 Spatial dispersal

In this stage, the produced seeds are circulated over the solution space by using the normally distributed random number with mean zero and changing standard deviation values. Due to the change in the variance value, the new seeds are distributed around the parent weed. The standard deviation (σ_{Gen}) of the distribution at the end of each generation reduces nonlinearly over the generations and is given as below:

$$\sigma_{\text{Gen}} = \frac{(\text{Gen}_{\max} - \text{Gen})^n}{(\text{Gen}_{\max})^n} \times (\sigma_{\text{initial}} - \sigma_{\text{final}}) + \sigma_{\text{final}} \tag{12}$$

where $\text{Gen}_{\max}$ is the maximum number of generations; σ_{Initial} and σ_{Final} represent the initial and final standard deviation, respectively; and n represents the modulation index.

To improve the performance of the algorithm, two terms known as the chaotic variable (Mohamadreza and Hamed 2012; Mojtaba et al. 2014) and cosine variable (Aniruddha et al. 2010; Roy et al. 2011) are added during the spatial dispersal phase. In IWO, the seeds are dispersed after the normal distribution. However, in the present problem, the chaotic random number is employed to distribute the seeds. This reduces the number of chances of the solution to be trapped in the local optimum while conducting the search. The chaotic random number used in the present study is given in Eq. 13.

$$X_{k+1} = \cos\left(k \cos^{-1}(X_k)\right) \tag{13}$$

For exploring the search space in an improved manner, the cosine term is added. The main aim of introducing the cosine term which is responsible for to increase the search space in a way such that it will utilize less resources. Once the cosine term is introduced, Eq. 14 can be restructured into the following form.

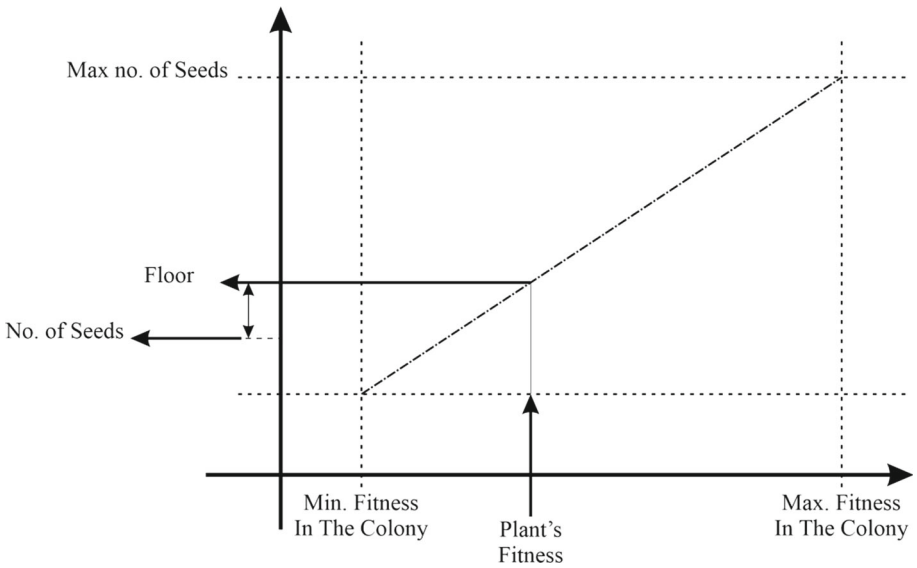

Fig. 5 Reproduction process in a colony of weeds

$$\sigma_{\text{Gen}} = \frac{(\text{Gen}_{\max} - \text{Gen})^n}{(\text{Gen}_{\max})^n} \times |\cos(\text{Gen})| \times (\sigma_{\text{initial}} - \sigma_{\text{final}}) + \sigma_{\text{final}} \tag{14}$$

3.3.4 Competitive exclusion

Finally, the developed seeds are grow into a flowering weed and are located in the weed colony along with the parent weeds and the elimination is performed based on the fitness value. Based on the fast reproduction of the seeds, the population size in the search space will cross its maximum limit ($P_{\max}$) after some generations. Once the maximum population ($P_{\max}$) is reached, the less fit weeds are excluded, and the weeds that have superior fitness are used for the subsequent generation. Further, the above procedure is repeated until the termination condition is reached.

4 Results and discussion

In the present research work, adaptive-based PID controllers are developed to control the motors mounted on the joints of the legs, that is, on both sagittal and frontal planes. To evaluate the performance of the proposed controller, simulation studies are conducted on the two-legged robot while moving on varying terrains—flat surface, ascending and descending the staircase, and sloped surface. Once the results of simulation are achieved, the gaits obtained by the adaptive controller are fed to the real two-legged robot to validate the results of simulation. The various parameters related to the two-legged robot are given in Table 1.

4.1 Performance tests

The performance assessment of the developed MCIWO methodology is tested by utilizing SPSS software. The said tests are conducted on a set of 5 benchmark functions with the dimension size of 10 (see Table 2) that are available in the literature (Mirjalili and Hashim 2010), and one real-world problem related to the development of an adaptive controller for the two-legged robot.

Table 1 Parameters related to the two-legged robot

Link	Length (m)	Mass (kg)	Inertia (kg-m^2)
Upper arm	0.060	0.1930	0.00008569
Lower arm	0.060	0.0592	0.00012000
Trunk	0.122	0.0975	0.00017700
Pelvis	0.037	0.1940	0.00671000
Upper limb of the leg	0.093	0.0700	0.00012600
Lower limb of the leg	0.093	0.1190	0.00007440
Ankle to foot	0.033	0.2460	0.00003300

The performance metrics related to the effectiveness, robustness and reliability of MCIWO are compared with IWO, PSO and DE (Mandava and Vundavilli 2018b) algorithms, respectively. The standard deviation and mean values of the said algorithms are given in Table 3. To compare the performance of the algorithms, the no. of iterations and average runs for which the algorithms need to run are kept fixed at 2000 and 30, respectively. It can be seen that the MCIWO approach is found to provide better values for standard deviation when compared to IWO, PSO and DE for the test functions 1, 3 and 4. But the test functions 2 and 5 are seen to provide slightly better value with the PSO algorithm when compared with the other two approaches. Moreover, the mean values of all the standard test problems of MCIWO approach are seen to outperform both the IWO and PSO methodologies.

4.2 Normality Test

In addition to the above performance tests, a normality test has also been conducted for 5 benchmark functions that specify the absence/presence of test of normality in the examined statistics. In the current research study, the authors have conducted two types of tests of normality such as Shapiro–Wilk (S–W) and Kolmogorov–Smirnov (K–S) which are used to examine the normality. In the above case study, the significance value level is kept equal at 0.05. However, the p value is found to be higher than the significance value. Based on the above reason, only the condition of normality is said to be fulfilled.

Here, the functions that are not fulfilling the condition of normality are denoted by symbol " + " in superscript. Moreover, it has also been observed that the functions 2 and 3 in PSO, 2 in DE, 1 and 10 in IWO and 1, 4 and 5 in MCIWO methodologies are seen to fulfill the condition of normality for both S-W and K-S methods (Table 4).

4.3 Parametric and nonparametric tests

In this research, the nonparametric and parametric tests, such as Wilcoxon and paired t-test, are conducted to check the pairwise statistical significance between MCIWO, IWO, DE and PSO algorithms. The significance level during these tests is taken as 0.05 for both the Wilcoxon and paired t-tests. Table 5 gives the results obtained during the above tests. The null hypothesis during the present study is kept fixed as follows: H_0: There is no variation in the performance of the algorithms developed; however, the alternative hypothesis is defined as follows: H_1: There is a

Table 2 The benchmark functions used in the present work

Function	Range
$F_1(y) = \sum_{i=1}^{n} y_i^2$	[− 100, 100]
$F_2(y) = \sum_{i=1}^{n-1} \left[100(y_{i+1} - y_i^2)^2 + (y_i - 1)^2\right]$	[− 30, 30]
$F_3(y) = \sum_{i=1}^{n} iy_i^4 + random[0, 1]$	[− 1.28, 1.28]
$F_4(y) = \sum_{i=1}^{n} \left[y_i^2 - 10\cos(2\pi y_i) + 10\right]$	[− 5.12, 5.12]
$F_5(y) = -20\exp\left(-0.2\sqrt{\frac{1}{n}\sum_{i=1}^{n} y_i^2}\right) - \exp\left(\frac{1}{n}\sum_{i=1}^{n}\cos(2\pi y_i)\right) + 20 + e$	[− 32, 32]

Table 3 Performance test results of PSO, IWO and MCIWO

Algorithms	F1	F2	F3	F4	F5
Mean					
PSO	4.66E-03	5.58514	1.81E-03	51.0080	2.50E-14
IWO	2.71E-05	4.08205	6.51E-04	13.4650	1.32E-04
DE	3.56E-03	4.56231	1.83 E-03	35.2356	1.89E-04
MCIWO	7.13E-06	3.90607	5.13E-04	9.4521	6.78E-05
SD					
PSO	1.34E-02	1.86000	1.05E-03	15.7227	4.28E-14
IWO	8.11E-06	1.80776	4.43E-04	6.07029	4.80E-05
DE	1.32E-03	2.28694	1.89E-03	10.2569	3.56E-05
MCIWO	2.17E-06	2.39114	2.63E-04	3.25039	2.19E-05

Table 5 The p values related to the paired t-test and Wilcoxon test

Algorithms	F1	F2	F3	F4	F5
T-test					
MCIWO-PSO	0.068	0.08	0.000	0.000	0.024
MCIWO-IWO	0.000	0.743	0.164	0.007	0.000
MCIWO-DE	0.000	0.076	0.000	0.004	0.032
Wilcoxon					
MCIWO-PSO	0.000	0.012	0.000	0.000	0.000
MCIWO-IWO	0.000	0.719	0.000	0.008	0.000
MCIWO-DE	0.002	0.085	0.005	0.005	0.002

variation in the performance of the algorithms developed in this study. More information related to this study is available in Derrac et al. (Derrac et al. 2011).

From Table 5, it can be observed that for test problems 1, 3, 4 and 5, the significance values are seen to be less than the value of p. From the above condition, it is concluded that the said test functions satisfy the signed rank test related to Wilcoxon test. Furthermore, for the function 2, the value of p is seen to be higher than the significance value and does not satisfy the Wilcoxon test.

In addition to the above study, paired t-test is also conducted on the said functions. The value of p for the test problems 1, 4 and 5 is realized to be smaller than the significance value for MCIWO with IWO. Moreover, the value of p for the test problems 1, 3, 4, 5 is less than the significance value for MCIWO and DE. Further, the paired t-test results between MCIWO and PSO for test problems 3, 4 and 5 show that their p values are realized to be smaller than the significance value. However, the values of p are less than 0.05 for function 5 in all the scenarios. Once the proposed MCIWO methodology is checked in terms of its convergence condition, the said approach is used to solve a real problem concerned with the tuning of PID controller of a two-legged robot while walking on a flat surface. Further, the results of this algorithm related to the two-legged robot have been compared with the help of the PSO based PID controller.

Table 4 The results related to the normality tests

	Test methods	F1	F2	F3	F4	F5
PSO	S-W test	$(0.000)^+$	(0.499)	(0.065)	$(0.029)^+$	$(0.034)^+$
	K-S test	$(0.000)^+$	(0.200)	(0.141)	(0.200)	(0.080)
DE	S-W test	$(0.032)^+$	(0.059)	$(0.034)^+$	(0.147)	$(0.005)^+$
	K-S test	$(0.023)^+$	(0.080)	$(0.000)^+$	(0.141)	(0.200)
IWO	S-W test	(0.234)	$(0.000)^+$	$(0.000)^+$	$(0.005)^+$	(0.113)
	K-S test	(0.200)	$(0.002)^+$	$(0.001)^+$	$(0.030)^+$	(0.147)
MCIWO	S-W test	(0.331)	$(0.035)^+$	$(0.048)^+$	(0.051)	(0.475)
	K-S test	(0.210)	$(0.004)^+$	(0.094)	(0.143)	(0.094)

Once the controller is designed, PID controller gains are tuned for the two-legged robot while walking on various surfaces by using the MCIWO-NN algorithm. Note that the prediction capability of NN highly depends on its architecture. A study was conducted to decide the number of hidden neurons in the hidden layer. The number of hidden neurons that provide better fitness when compared with other structures is observed to be 16. The number of input and output neurons that correspond to the inputs and outputs of the process are observed to be 12 and 36, respectively. The number of connecting weights in the network is found to be equal to 768 ($12 \times 16 + 16 \times 36$). Moreover, two bias values one for the hidden and output layers each are introduced into the network. Therefore, the total number of variables required to optimize the structure of NN is 770. While solving the problem in the present study, the connecting weights are varied between 0.0 and 1.0, and the bias values are varied between 0.0 and 0.0001. In addition to the above variables, the coefficients of transfer functions, that is, linear, tan-sigmoid, and log-sigmoid that correspond to the input, hidden, and output layers, respectively, are also included in the string. A parametric study is conducted to determine the optimal parameters of the MCIWO algorithm that optimizes the structure of NN. While conducting a parametric study, the input parameters related to the proposed algorithm, that is, the initial population, final population, modulation index, maximum and minimum number of seeds, final and initial standard deviation, and number of generations, are kept fixed at 5, 15, 3, 5, 0, 0.00001, 3 and 20. The optimal parameters related to the MCIWO algorithm while the two-legged robot moving on various terrains are listed in Table 6.

Once the optimal structure for the MCIWO-NN-based PID controller was obtained, a comparative study was conducted for the two-legged robot in terms of the angular error, average torque required at various joints, ZMP, and dynamic balance margin of the two-legged robot while walking on various terrains.

Table 6 Optimal parameters related to the MCIWO algorithm while the two-legged robot is walking on various surfaces

Parameters	Flat surface	Ascending		Descending	
		Stair	Slope	Stair	Slope
$\sigma_{initial}$	4%	4%	4%	4%	3%
n	5	4	3	2	4
S_{max}	6	4	6	2	8
$npop_f$	25	10	8	15	10
Gen	80	50	60	70	60

The error magnitude corresponding to the various joints of the swing and stance legs of the two-legged robot is displayed in Fig. 6. For all the joints, the magnitude of error is very high initially and decreases slowly with time interval. The main aim of this research work is to minimize the error between the actual and desired torque. It can also be observed that the error is minimized in the range of ± 0.07 for all the joints within 4 to 5 ms time interval. Moreover, the error generated at various successive joints of the two-legged robot while walking on a flat surface is less than that generated when the two-legged robot is ascending and descending on a staircase and sloped surface. This phenomenon may be due to the difference between the two subsequent angles of a two-legged robot's joint is low while walking on a flat surface as compared with that between the two subsequent angles of a two-legged robot's joint while walking on other surfaces.

Figure 7 displays the torque required at various joints of the two-legged robot while walking on various terrains. The average torque required is seen to be more while ascending the staircase and less while walking on a flat surface. This may be because the angular variation between the successive joints is more while ascending the staircase. Furthermore, the torque required at joint 3 is high when compared with the torque required at the other joints of the two-legged robot. The reason of this difference may be that joint 3 carries other links and joints of the two-legged robot while moving the swing leg from one position to another. It might have occurred due to the large angular displacement obtained at that joint. This assumption is verified from the error plots in which the convergence requires more time (Fig. 5b).

The variation of the ZMP location in the foot support polygon for the two-legged robot while walking on a flat surface, ascending and descending a staircase, and sloped surface are displayed in Fig. 8. The position of ZMP is observed to lie inside the foot support polygon for all the cases. Therefore, the motion of the two-legged robot is considered to be dynamically balanced in all the cases. The flat surface movement of the two-legged robot is observed to be more balanced as the location of the ZMP for the flat surface walk is closer to the center of the support foot as compared with the location of the ZMP for all other walks (that is, ascending and descending the staircase and sloped surface). The location of ZMP is slightly away from the center of the foot support polygon for the sloped surface walking compared with the location of ZMP for the flat surface and staircase walking. This might be due to the fact that in the case of the sloped surface, the projection of the foot support is considered instead of the length of the foot (that is, foot is along the slope surface) to determine the location of ZMP. Therefore, the location of ZMP for the sloped surface walking is pushed away from the center of

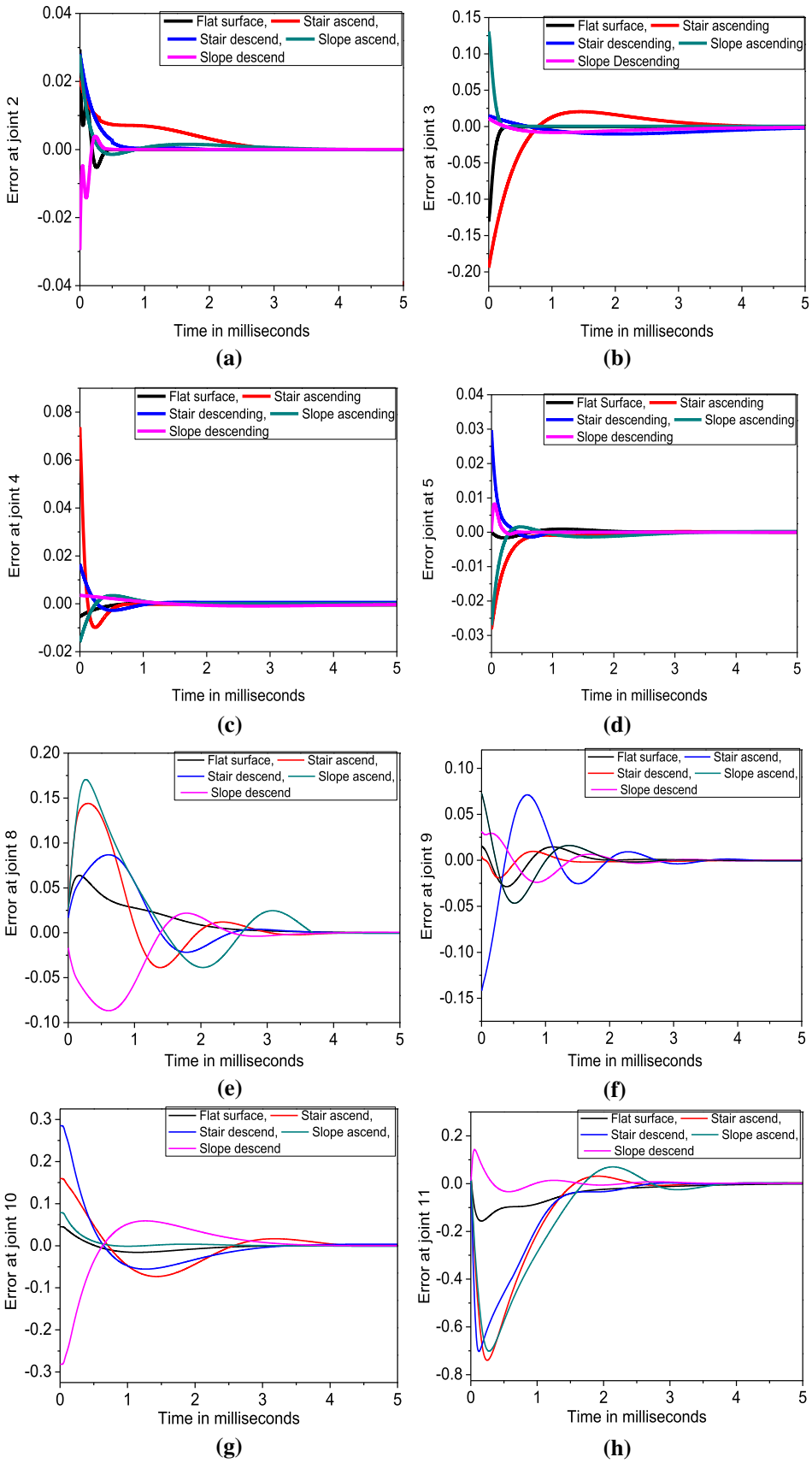

Fig. 6 Variation of the angular error at various joints: **a** joint 2, **b** joint 3, **c** joint 4, **d** joint 5, **e** joint 8, **f** joint 9, **g** joint 10, and **h** joint 11

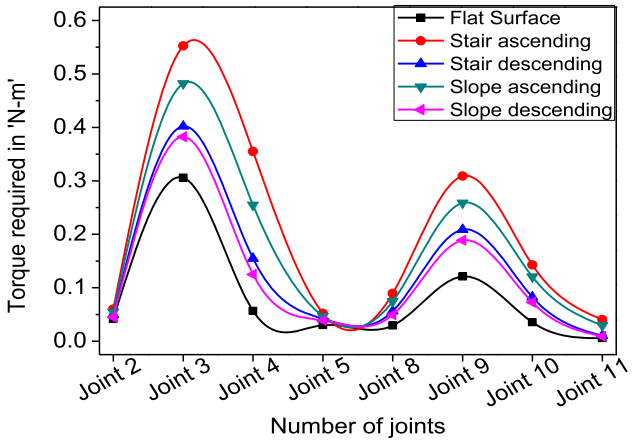

Fig. 7 Variation of torque required at different joints

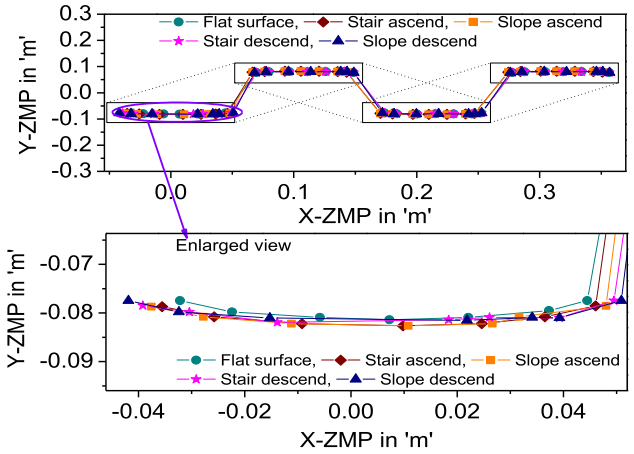

Fig. 8 Variation of the ZMP in the X and Y directions

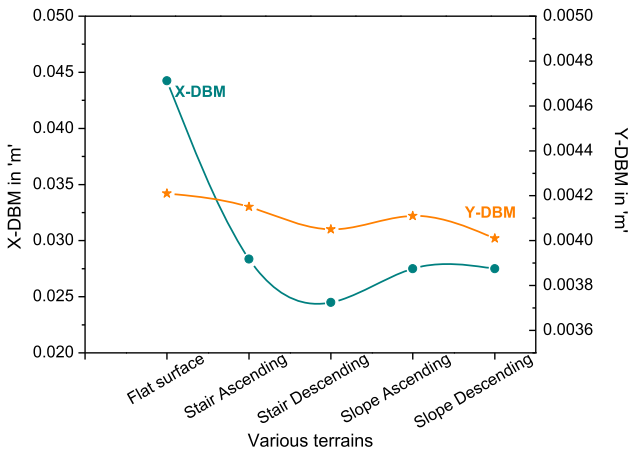

Fig. 9 Average X and Y DBM on various terrains

the foot when compared with the flat surface and staircase walking. This fact has also been confirmed from Fig. 9, which shows the variation of DBM in the X and Y directions. The DBM is determined by the location of ZMP from the end of the foot support polygon. The flat surface gait provides high balance values for the X and Y directions when compared with that provided by other walking cases (that is, staircase and sloped surfaces). This observation matches with the natural walking behavior of human beings on the specified terrains. The reason for this is the same as the one explained above.

After conducting the simulations and observing the performance of the adaptive controller, the gait angles generated by various joints of the two-legged robot are fed into the real two-legged robot to evaluate the practical performances. All the aforementioned gaits are dynamically balanced in nature. Moreover, Figs. 10, 11, 12, 13, and 14 display the two-legged robot walking on flat surface, ascending and descending the staircase, and sloped surfaces at various instances.

4.4 Comparison with previous studies

In the present study, the authors have conducted a quantitative and qualitative comparison with the works available in the literature. The results of quantitative comparison of the proposed algorithm with the algorithms available in the literature such as, PSO and MCIWO (Mandava and Vundavilli 2018a) are shown in Fig. 15. It can be observed that the MCIWO-NN-based adaptive controller is found to consume less amount of torque when compared with other algorithms namely, PSO, MCIWO (Mandava and Vundavilli 2018a) and PSO-NN algorithm on all terrain conditions.

In the literature (Shih 1999; Huang et al. 2001; Chiang and Chiang 2013; Vundavilli and Pratihar 2011; Mousavi and Bagheri 2007; Ranjbar and Mayorga 2017; Bagheri et al. 2010), the researchers considered a 7-DOF two-legged robot for generating gaits on various surfaces, and they only used the analytical approach to solve the related problems. In this study, the authors not only considered the gait generation algorithm on various terrains but also designed an adaptive-based PID controller (that is, MCIWO-NN) that helps in gait execution in a smooth manner. In addition to the above statement, the investigators in Jimenez et al. (2013), Aghbali and Koma (2013b), Kajita et al. (2010), Park et al. (2009), Engelbrecht (2007) developed a ZMP-based PID controller, which is an indirect way of controlling the motors mounted on the joints of the two-legged robot. However, in the present study, the authors developed a torque-based PID controller, which directly caters to the error in the angular displacements of the motors. Moreover, in Yau et al. (2008), Hang et al. (2002), Fister et al. (2016), Varol and Bingul (2004), the researchers used an evolutionary algorithm that could provide only one set of gain values for the controller for tuning it. In the present research, the authors have developed an adaptive-torque-based PID controller that can

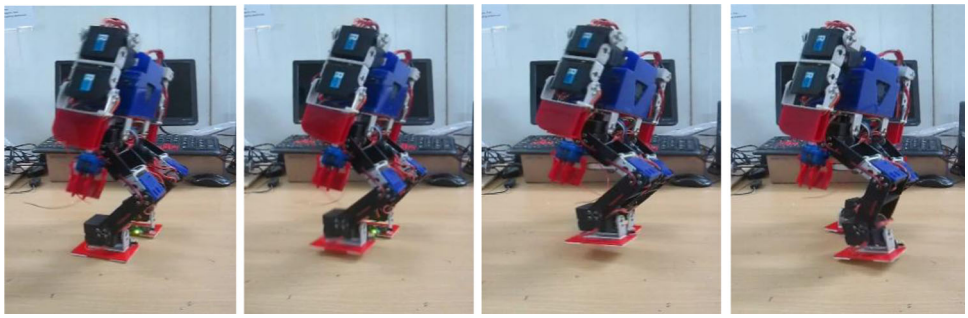

Fig. 10 Two-legged robot walking on a flat surface

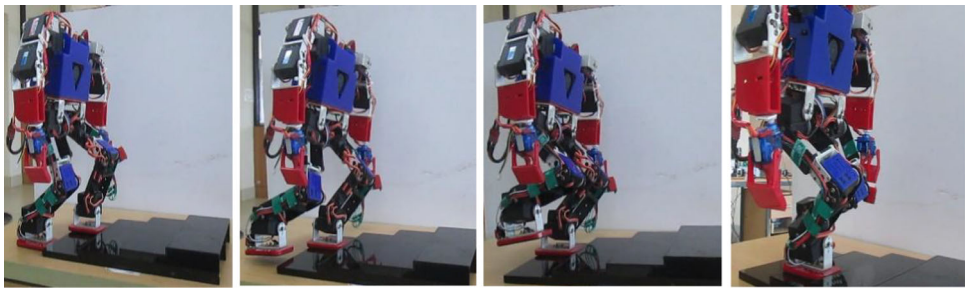

Fig. 11 Two-legged robot ascending a staircase

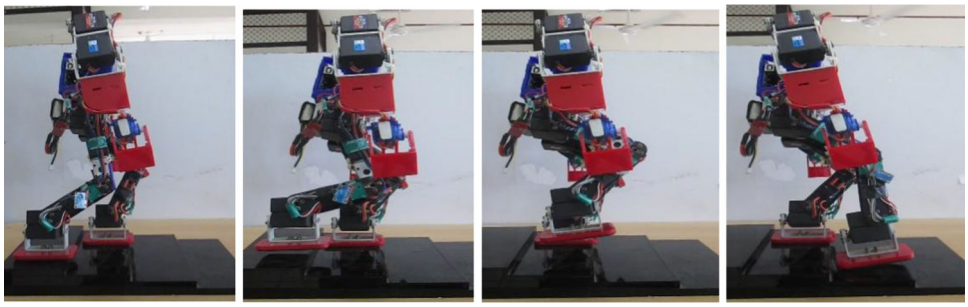

Fig. 12 Two-legged robot descending a staircase

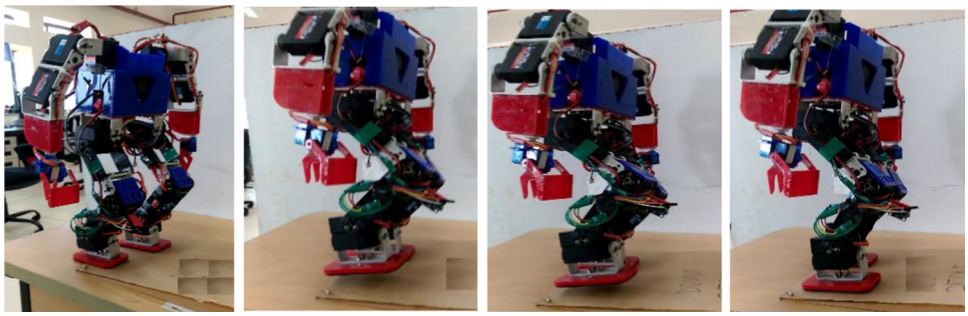

Fig. 13 Two-legged robot walking on ascending the sloping surface

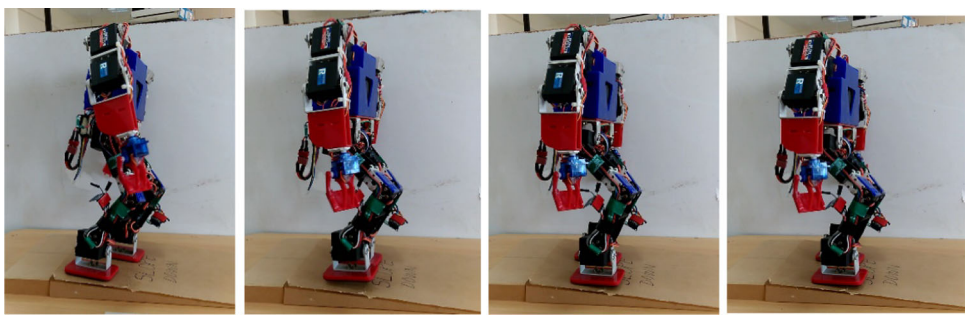

Fig. 14 Two-legged robot walking on a descending sloped surface

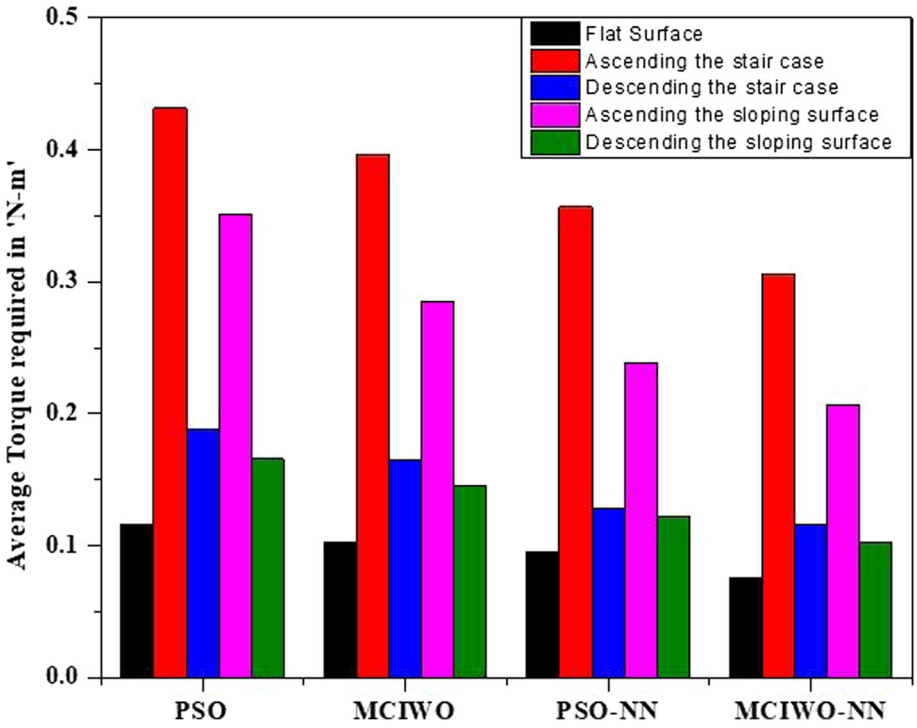

Fig. 15 Schematic diagram showing the comparison of average torque required for various algorithms

produce variable gains based on the magnitude of the error signal at the controllers input.

5 Conclusions

The present paper has successfully developed an innovative MCIWO-NN-based adaptive PID controller for real-time applications for two-legged robot walking on various terrains. The results demonstrate that the proposed adaptive-based PID controller can learn the highly nonlinear and dynamic features of the two-legged robotics and quickly reduce the tracking error to zero when it is walking on a flat surface. Moreover, while ascending and descending a staircase and while walking on a sloped surface, the tracking error reduces to zero after a few milliseconds. The torque required, and dynamic balance margin of the two-legged robot is high while the robot ascends the staircase and moves on a flat surface, respectively. Moreover, the proposed MCIWO-NN-based PID controller is capable of modifying the PID parameters K_p, K_d, and K_i in real time, and the actual gait can be monitored. The results of the algorithm are validated on a real two-legged robot. Further, this work can also be extended to cross a ditch, avoiding obstacle, walking on a rough terrain filled with sand and stones. In the present work, no damping effect is considered between the foot–ground interactions of the biped robot while landing its swing foot. This may cause the vibrations to transmit into the body of the robot and may influence the dynamic balance of the biped robot. Therefore, in future attempts will be made to model the foot–ground interaction as a multi-DOF system to have a smooth walk of the biped robot on various terrains.

Funding There is no funding agency supported for completing this research work.

Declarations

Conflict of interest Author A declares that he/she has no conflict of interest. Author B declares that he/she has no conflict of interest.

Ethical approval This article does not contain any studies with human and animal participants performed by any of the authors.

References

Affolter K, Hanne T, Schweizer D, Dornberger R (2016) Invasive weed optimization for solving index tracking problems. Soft Comput 20(9):3393–3401. https://doi.org/10.1007/s00500-015-1799-x

Aghbali B, Koma AYO (2013a) ZMP trajectory control of a humanoid robot using different controllers based on an offline trajectory generation. In: Proceeding of the 2013 RSIIISM international conference on robotics and mechatronics, Tehran, Iran, pp 530–534

Aghbali B, Koma AY (2013b) ZMP trajectory control of a humanoid robot using different controllers based on an offline trajectory

generation. In: Proceeding of the 2013 RSIIISM international conference on robotics and mechatronics, Tehran, Iran
Anh HPH, Huan TT, Nam NT (2014) Novel robust walking for biped robot using adaptive neural PID controller. In: International conference on automatic control theory and application, pp 86–89
Aniruddha B, Siddharth P, Swagatam D, Ajith A (2010) A modified invasive weed optimization algorithm for time-modulated linear antenna array synthesis. IEEE Cong Evolut Comput 1–10.
Bagheri A, Miripour-Fard B, Mousavi PN (2010) Mathematical modelling and simulation of combined trajectory paths of a seven link biped robot. Climb Walk Robot
Bouhajar S, et al (2015) Trajectory generation using predictive PID control for stable walking humanoid robot. In: Procedia computer science, the international conference on advanced wireless, information, and communication technologies, pp 86–93.
Cheng MY, Lin CS (2000) Dynamic bio-robotic leg locomotion on less structured surfaces. Robotica 18:163–170
Chiang MH, Chiang R (2013) Anthropomorphic design of the human-like walking robot. J Bionic Eng 10:186–193
Chu Z, Sun F, Cui J (2008) Disturbance observer-based robust control of free-floating space manipulators. IEEE Syst J 2(1):114–119
Clever D, Hu Y, Mombaur K (2018) Humanoid gait generation in complex environments based on template models and optimality principles learned from human beings. Robot Res 37(10):1–20
Derrac J, Garcia S, Molina D, Herrera F (2011) A practical tutorial on the use of nonparametric statistical tests as a methodology for comparing evolutionary and swarm intelligence algorithms. Swarm Evolut Comput 1:3–18
Engelbrecht AP (2007) Computational intelligence. In: An introduction. Wiley, Hoboken.
Fister D, Fister I, Fister I, Safaric R (2016) Parameter tuning of PID controller with reactive nature-inspired algorithms. Robot Autonom Syst 84:64–75
Hang CC, Astrom KJ, Wang QG (2002) Relay feedback auto-tuning of process controllers. A Tutor Rev J Process Control 12(1):143–162
Hojati M, Gazor S (2002) Hybrid adaptive fuzzy identification and control of nonlinear systems. IEEE Trans Fuzzy Syst 10(2):198–210
Huang Q, Yokoi K, Kajita S, Kaneko K, Arai H, Koyachi N, Tanie K (2001) Planning walking patterns for a biped robot. IEEE Trans Robot Autom 17:280–289
Jimenez JJA, Perez DH, Barbera HM (2013) A simple feedback controller to reduce angular momentum in ZMP-based gaits. Int J Adv Robot Syst 10:1–7
Juang JG (2001) Intelligent trajectory control using recurrent averaging learning. Appl Artif Intell 15(3):277–296
Kajita S, et al (2010) Biped walking stabilization based on linear inverted pendulum tracking. In: The 2010 IEEE/RSJ international conference on intelligent robots and systems, Taipei, Taiwan, pp 4489–4496
Kajita S (2017) Feedback control of inverted pendulums. In: Goswami A, Vadakkepat P (eds) Humanoid robotics: a reference. Springer, Dordrecht
Kajita S, Morisawa M, Miura K, Nakaoka S, Harada K, Kaneko K, Kanehiro F, Yokoi K (2010) Biped walking stabilization based on linear inverted pendulum tracking. In: The 2010 IEEE/RSJ international conference on intelligent robots and systems, Taipei, Taiwan
Kelly R, Santibáñez V, Loría A (2005) Control of robot manipulators in joint space. Springer, London
Koker R, Cakar T, Sari Y (2014) A neural-network committee machine approach to the inverse kinematics problem solution of robotic manipulators. Eng Comput 30(4):641–649
Londhe PS, Patre BM (2018) Adaptive fuzzy slidingmode control for robust trajectory tracking control of an autonomous underwater vehicle. Intell Service Robot. https://doi.org/10.1007/s11370-018-0263-z
Malekabadi M, Haghparast M, Nasiri F (2018) Air condition's PID controller fine-tuning using artificial neural networks and genetic algorithms. Computers 7:1–14
Mandava RK, Vundavilli PR (2018a) Near optimal PID controllers for the biped robot while walking on uneven terrains. Int J Autom Comput 15(6):689–706
Mandava RK, Vundavilli PR (2018b) Implementation of modified chaotic invasive weed optimization algorithm for optimizing the PID controller of the biped robot". Sādhanā 43(5):1–18
Mehrabian AR, Lucas C (2006) A novel numerical optimization algorithm inspired from weed colonization. Ecol Inform 1(4):355–366
Mirjalili S, Hashim SZM (2010) A new hybrid PSOGSA algorithm for function optimization. Int Conf Comput Inform Appl (ICCIA 2010), pp 374–377.
Mohamadreza A, Hamed M (2012) Chaotic invasive weed optimization algorithm with application to parameter estimation of chaotic systems. Chaos Solitons Fract 45:1108–1120
Mojtaba G, Sahand G, Jamshid A, Mohsen G, Hasan F (2014) Application of chaos-based chaotic invasive weed optimization techniques for environmental OPF problems in the power system. Chaos Solitons Fract 69:271–284
Mousavi PN, Bagheri A (2007) Mathematical simulation of a seven link biped robot on various surfaces and ZMP considerations. Appl Math Model 31:18–37
Naidu YR, Ojha AK (2015) A hybrid version of invasive weed optimization with quadratic approximation. Soft Comput 19(12):3581–3598. https://doi.org/10.1007/s00500-015-1896-x
Nguyen T, Tao L, Hasegawa H (2016) Gait generation for a small biped robot using approximated optimization method. In: Proceedings of the 2016 second international conference on mechanical engineering and automation science, IOP conference series: materials science and engineering, vol 157, pp 1–5.
Park S, Han Y, Hahn H (2009) Balance control of a biped robot using camera image of reference object. Int J Control Autom Syst 7(1):75–84
Ranjbar M, Mayorga RV (2017) A seven link biped robot walking pattern generation on various surfaces. Wseas Trans Syst 16:299–312
Roy GG, Das S, Chakraborty P, Suganthan PN (2011) Design of non - uniform circular antenna arrays using a modified invasive weed optimization algorithm. IEEE Trans Anten Propag 59(1):110–118
Satoh S, Fujimoto K (2018) Gait generation for a biped robot with knees and torso via trajectory learning and state-transition estimation. Artif Life Robot 23(4):489–497
Shamna P, Priya N, Ahamed KS (2017) Walking stability control of biped robot based on three mass with angular momentum model using predictive PID control. In: International conference on electronics, communication and aerospace technology ICECA 2017, Coimbatore, India, pp 584-588
Shih CL (1999) Ascending and descending stairs for a biped robot. IEEE Trans Syst Man Cybern A Syst Hum 29:255–268
Slotine JE, Li W (1991) Applied nonlinear control. Prentice-Hall, Englewood Cliffs
Varol HA, Bingul Z (2004) A new PID tuning technique using ant algorithm. In: Proceeding of the 2004 American control conference, Boston, Massachusetts
Vukobratovic M, Borovac B (2004) Zero-moment point: thirty-five years of life. Int J Hum Robot 1(1):157–173
Vundavilli PR, Pratihar DK (2011) Balanced gait generations of a two-legged robot on sloping surface. Sadhana 36(4):525–550

Wai RJ, Muthusamy RK (2013) Fuzzy-neural-network inherited sliding mode control for robot manipulator including actuator dynamics. IEEE Trans Neural Netw Learn Syst 24(2):274–287

Wang L et al (2013) Energy-efficient SVM learning control system for biped walking robots. IEEE Trans Neural Netw Learn Syst 24(5):831–837

Wu HM, Hwang CL (2011) Trajectory-based control under ZMP constraint for the 3D biped walking via fuzzy control. In: IEEE international conference on fuzzy systems, Taipei, Taiwan, pp 706-712

Wu Y, Song Q, Yang X (2007) Robust recurrent neural network control of biped robot. J Intell Robot Syst 49:151–169

Yau TJ, Yun TC, Chih PH (2008) Design of fuzzy PID controllers using modified triangular membership functions. J Inform Sci 178(12):1325–1333

Yoo SJ, Park JB, Choi YH (2007) Robust control of planar biped robots in single support phase using intelligent adaptive back stepping technique. Int J Control Autom Syst 5(3):269–282

Zang X, Liu Y, Liu X, Zhao J (2016) Design and control of a pneumatic musculoskeletal biped robot. Technol Health Care 24:S443–S454